

# Sub-monolayer Au<sub>9</sub> Cluster Formation via Pulsed Nozzle Cluster Deposition

*Jesse Daughtry,<sup>1,2</sup> Gregory F. Metha,<sup>4</sup> Siriluck Tesana,<sup>5</sup> Tomonobu Nakayama<sup>3\*</sup> and  
Gunther G. Andersson,<sup>1,2\*</sup>*

<sup>1</sup> Flinders Institute for NanoScale Science and Technology, Flinders University, Adelaide SA 5001, Australia

<sup>2</sup> Flinders Microscopy and Microanalysis, College of Science and Engineering, Flinders University, Adelaide, SA 5042, Australia

<sup>3</sup> National Institute for Materials Science, 1-1 Namiki, Tsukuba, Ibaraki 305-0044, Japan

<sup>4</sup> Department of Chemistry, The University of Adelaide, Adelaide, SA 5005, Australia

<sup>5</sup> The MacDiarmid Institute for Advanced Materials and Nanotechnology, School of Physical and Chemical Sciences, University of Canterbury, Christchurch 8041, New Zealand.

## Corresponding Author

\*Email: (G.G.A.) [gunther.andersson@flinders.edu.au](mailto:gunther.andersson@flinders.edu.au)

\*E-mail: (T.N.) [nakayama.tomonobu@nims.go.jp](mailto:nakayama.tomonobu@nims.go.jp)

## Supporting Information

S1-3: AFM scans on B-series samples showing areas of high cluster concentration indicating sub-optimal depositions

S4: AFM scans on Mica control samples showing non-optimal control depositions

S5: High resolution XPS scan at the Au 4f region on a partially agglomerated sample.

S6: AFM scans and particle analysis on Sample B6

S7: AFM scans showing the ability of AFM tip to move deposited gold clusters on a mica surface

S8: TEM and EDX indicating the presence of Au in the PNCD-prepared samples

S9: High resolution XPS showing the C deposited through PNCD and it's removal through subsequent heating

S10: Mathematica code for the modelling of PNCD

S11: AFM showing the results of PNCD of Au55/101 onto ALD TiO<sub>2</sub> producing similarly disperse coverages of gold cluster sized particles.

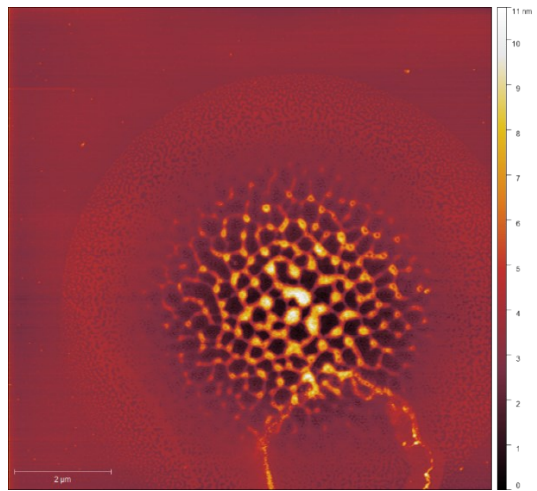


Figure S1 0.125mM Au<sub>9</sub>/methanol, 30x pulses, 250μs, Sample B4

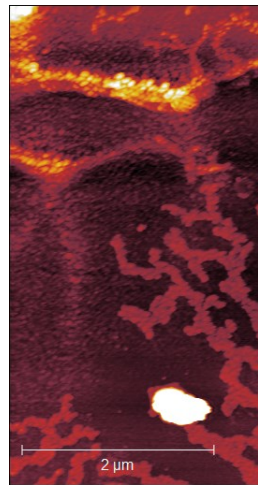


Figure S2 0.125mM Au<sub>9</sub>/methanol, 100x pulses, 250μs, Sample B1

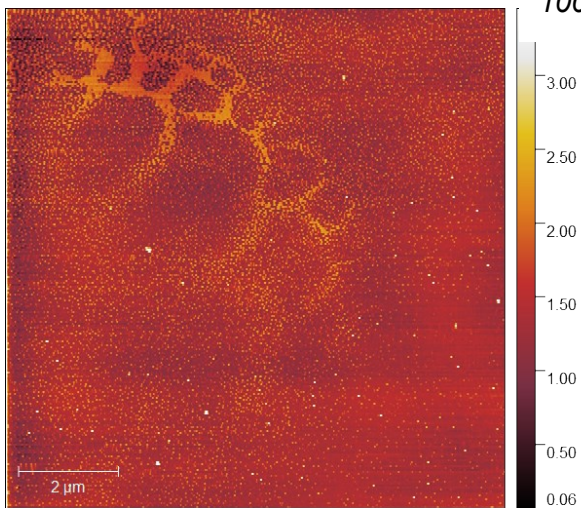


Figure S3 0.04 mM Au<sub>9</sub>/methanol, 10x pulses, 150μs

Figures S1-S3 show a range of non-optimised depositions resulting in monolayer or higher coverages of the gold clusters. This range shows depositions from high pulse numbers that produce very high coverage and appearance of surface structures attributed to droplet impacts on the surface, even with low pulse width (opening time). This was attributed to

continued pulsing allowing larger droplets to form and reach the substrate before vaporisation.

Improved dispersion and reduced droplet-like features were observed with the use of larger pulse width and lower pulse numbers. Pulse time was determined through iterations, 100 $\mu$ s was too short for observable pressure increases on pulsing. Increased in 50 $\mu$ s steps until stable pressure increases observed around 250 $\mu$ s and droplet-like features were no longer observed, this was used as the experimental pulse width.

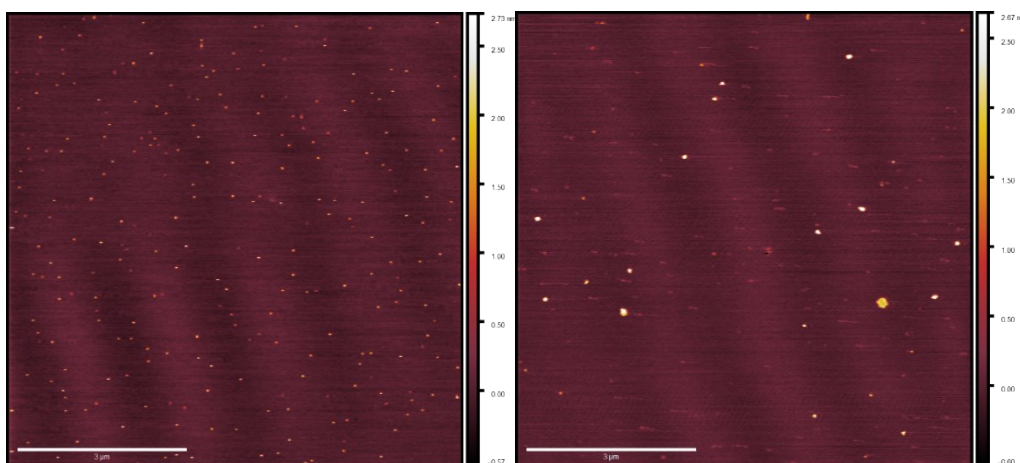


Figure S4. AFM scans of mica control images showing a methanol-only (no cluster) deposition that resulted in partial removal of the particles seen in fresh cleaved mica samples and some larger particles/residue (approx. 10-20 nm high) across the surface. This was only seen in this sample and was attributed to sub-optimal depositions conditions.

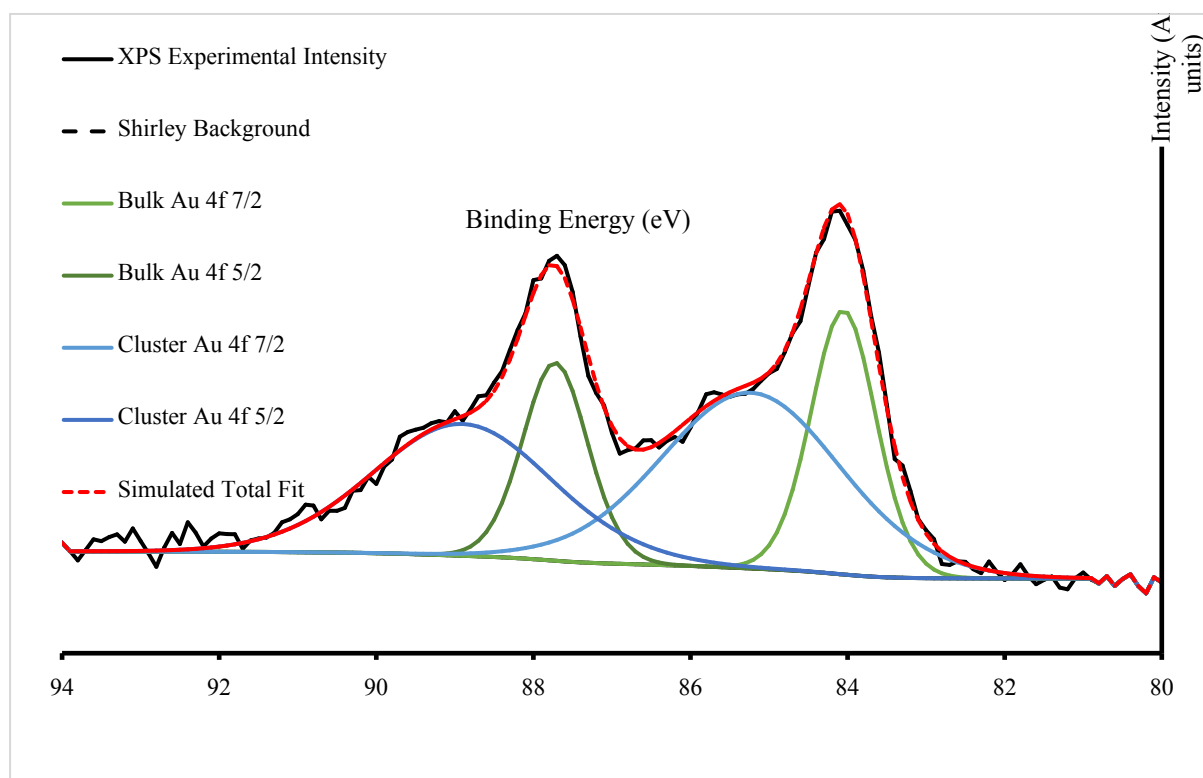


Figure S5. High resolution XPS scan at the Au 4f region. 2 distinct species are evident with gold cluster  $4f_{7/2}$  Au peak at 85 eV while bulk Au peak can be seen at 84.2 eV showing that some cluster agglomeration has occurred.

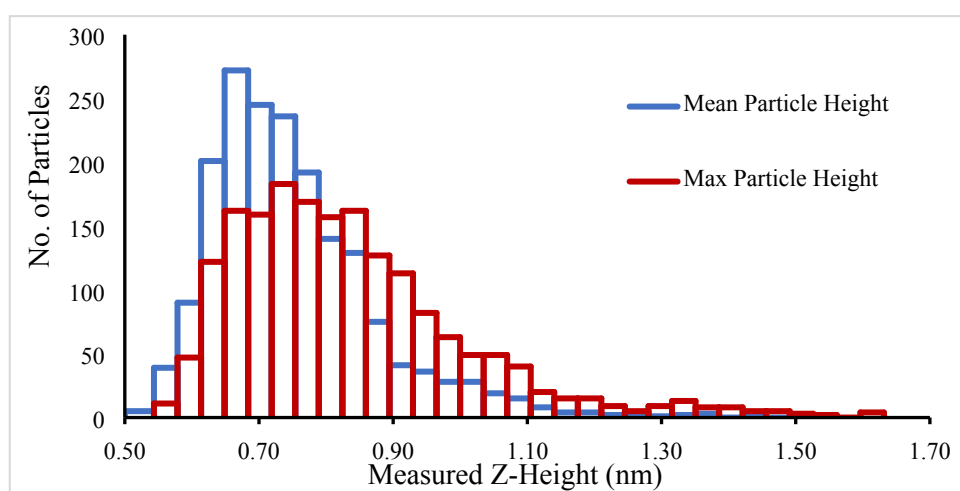
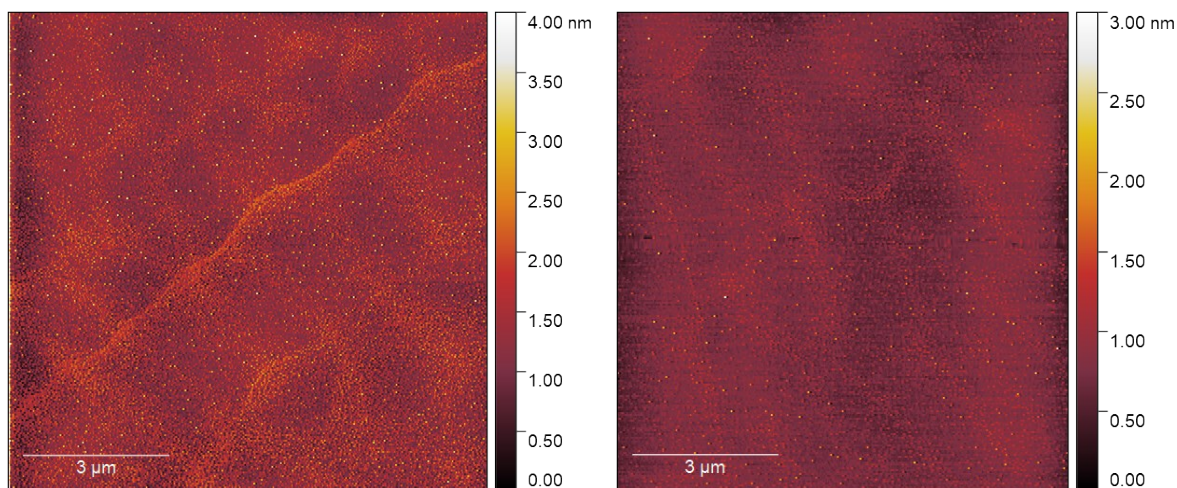
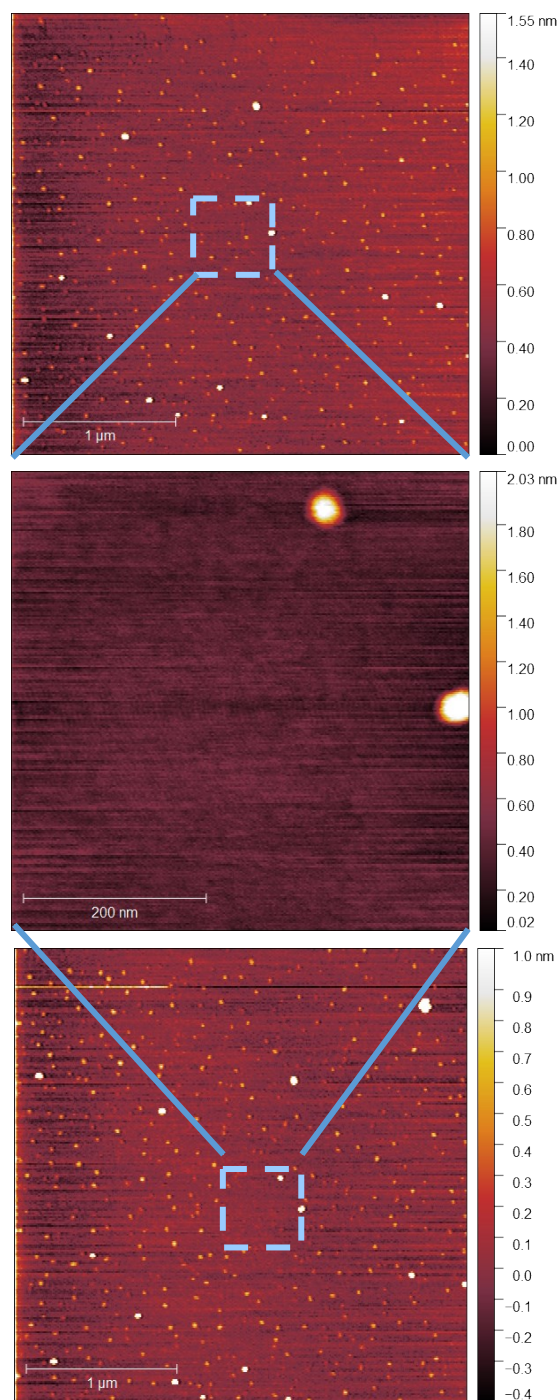


Figure S6. AFM scans of sample B6 (on mica) at different locations showing largely homogenous depositions of cluster sized particles with no droplet-like features. Bottom - Particle height distribution for 10  $\mu\text{m}$  scan of sample B6 show the weighting of maximum and mean particle heights for each scan, with the distributions for both in agreement for large numbers of sub-nanometer (gold cluster sized) particles. Lateral measurements are not accurate for AFM but height profile matches  $\text{Au}_9$  gold cluster. single pulse deposition showing major distribution of deposited particles between 0.65-0.91nm.



*Figure S7 AFM scans of pulsed vapour deposited Au<sub>9</sub> onto Mica. All scans were performed at the same location with top and bottom being 3µm<sup>2</sup> and middle being 500nm<sup>2</sup>. The blue frame indicates common scan regions. The top and bottom images are 3µm<sup>2</sup> AFM scans taken before (top) and after (bottom) the central 500nm<sup>2</sup> scan.*

AFM scans seen in Fig.7 illustrate the evidence for cluster manipulation/mobility under AFM. The cluster sized objects in the top scan are not evident in the centre scan and once the large scan was repeated in the bottom scan it was evident these clusters had been pushed to the frame edge by the AFM tip.

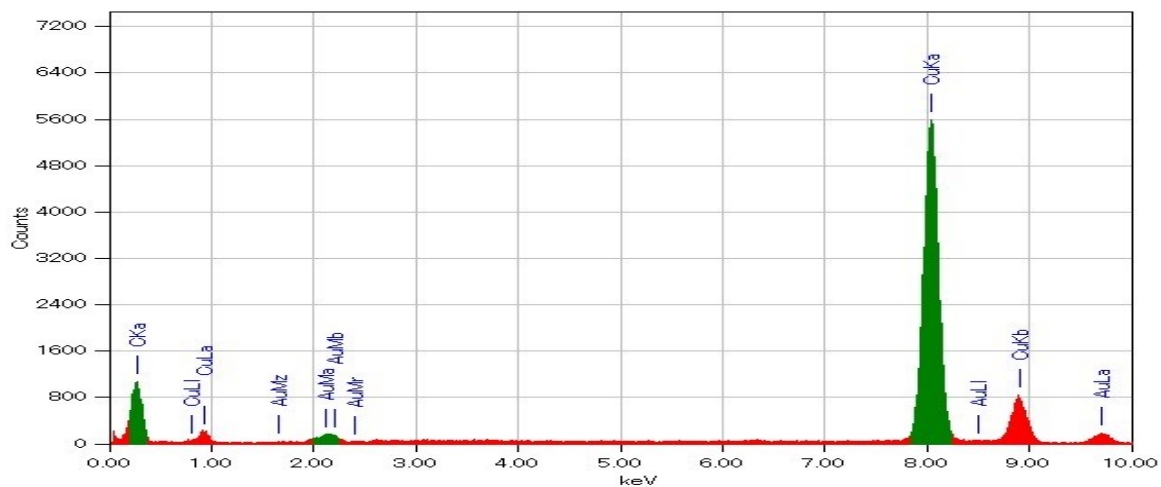
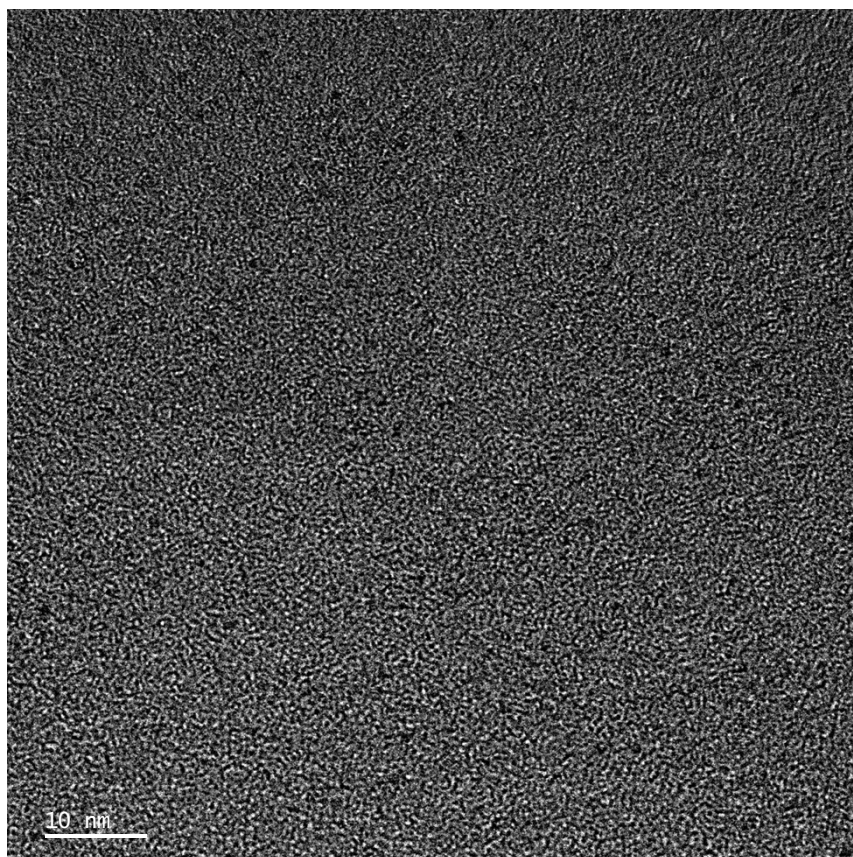


Figure S8: TEM scan on a 40x pulse deposited 0.125mM Au<sub>9</sub>/Methanol sample using amorphous carbon microgrid. The top part shows a TEM scan of a PNCD deposition on to carbon microgrid with a region of dense coverage of metallic species. The bottom part shows the EDX result. Au was found (~ 2.1 keV) on this sample. In other TEM samples the Au concentration was below the threshold for detection using EDX. Cu signal seen in the EDX comes from the microgrid structure.

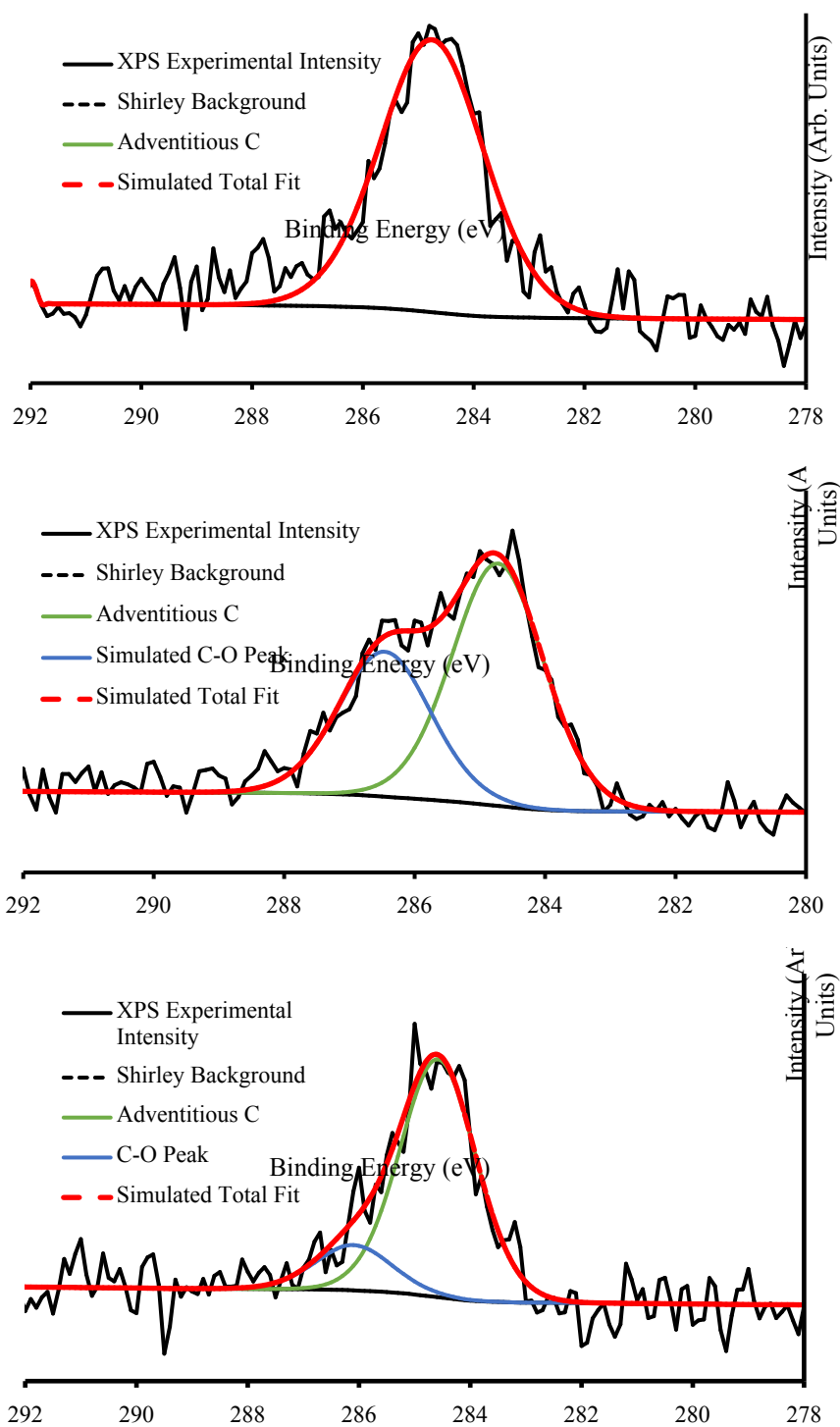


Figure S9. The carbon peaks in XPS show A) a cleaned surface B) the growth of a C peak with 3 pulses of  $Au_9$ /Methanol C) After heating to 200°C, the C peak appearing with deposition is almost completely removed.

```

In[ ]:= f = e-A / r ;

In[ ]:= γ = .0225; (*surface tension*)
Ω = 1.76 × 10-28; (*molecular volume*)
k = 1.38 × 10-23; (*Boltzmann's Const.*)
T = 300; (*Temperature*)
m = 1.53 × 10-25; (*molecular mass (evap. particle)*)
p = 18870; (*partial pressure of flat surface*)
A =  $\frac{2 * \gamma * \Omega}{k * T}$ ;
B =  $\frac{\sqrt{2 * \pi * m * k * T}}{\Omega * p}$ ;
rf = 3.5 × 10-10;
ro = 0.00001;

In[ ]:= tev = B * (Integrate[f, {r, rf, ro}])
Out[ ]:= 0.000189629

In[ ]:= ScientificForm[tev]
Out[ ]//ScientificForm=
1.89629 × 10-4

In[ ]:= NumberForm[0.000189629]
Out[ ]//NumberForm=
0.000189629

In[ ]:= ClearAll[ρ, ΔP, d, L, F, g, v, x]

In[ ]:= ρ = 791 kg/m3; (*density of Methanol, kg/m^3*)
ΔP = UnitConvert[202700 Pa]; (*pressure drop from nozzle head to chamber, Pa*)
 $\frac{\Delta P}{\rho}$ 
d = 0.51 mm; (*nozzle diameter, meters*)
L = UnitConvert[1.25 mm]; (*nozzle orifice length, meters*)
F = 0.035; (* reynolds number 104, drawn steel,
stainless steel roughness 0.0015mm roughness,
https://www.nuclear-power.net/nuclear-engineering/fluid-dynamics/major-head-loss-friction-loss/friction-factor-turbulent-flow-colebrook/,
http://www.calctool.org/CALC/eng/civil/friction\_factor*)
F *  $\frac{L}{d}$ 
g = 9.8 m/s2; (*gravitational constant, newton square meters per kilogram squared*)

Out[ ]:=  $\frac{202700}{791} \text{ m}^2/\text{s}^2$ 
Out[ ]:= 0.0857843

In[ ]:= Sqrt[ $\frac{\Delta P}{\rho} / F * \frac{L}{d} * \frac{1}{2g}$ ]
Out[ ]:= 30.2584 √m

In[ ]:= 30.258 m/s * 0.000189629` s
Out[ ]:= 0.00573779 m

```

Figure S10: Mathematica code used to model the PNCD evaporation time and velocity, useable code available on request.

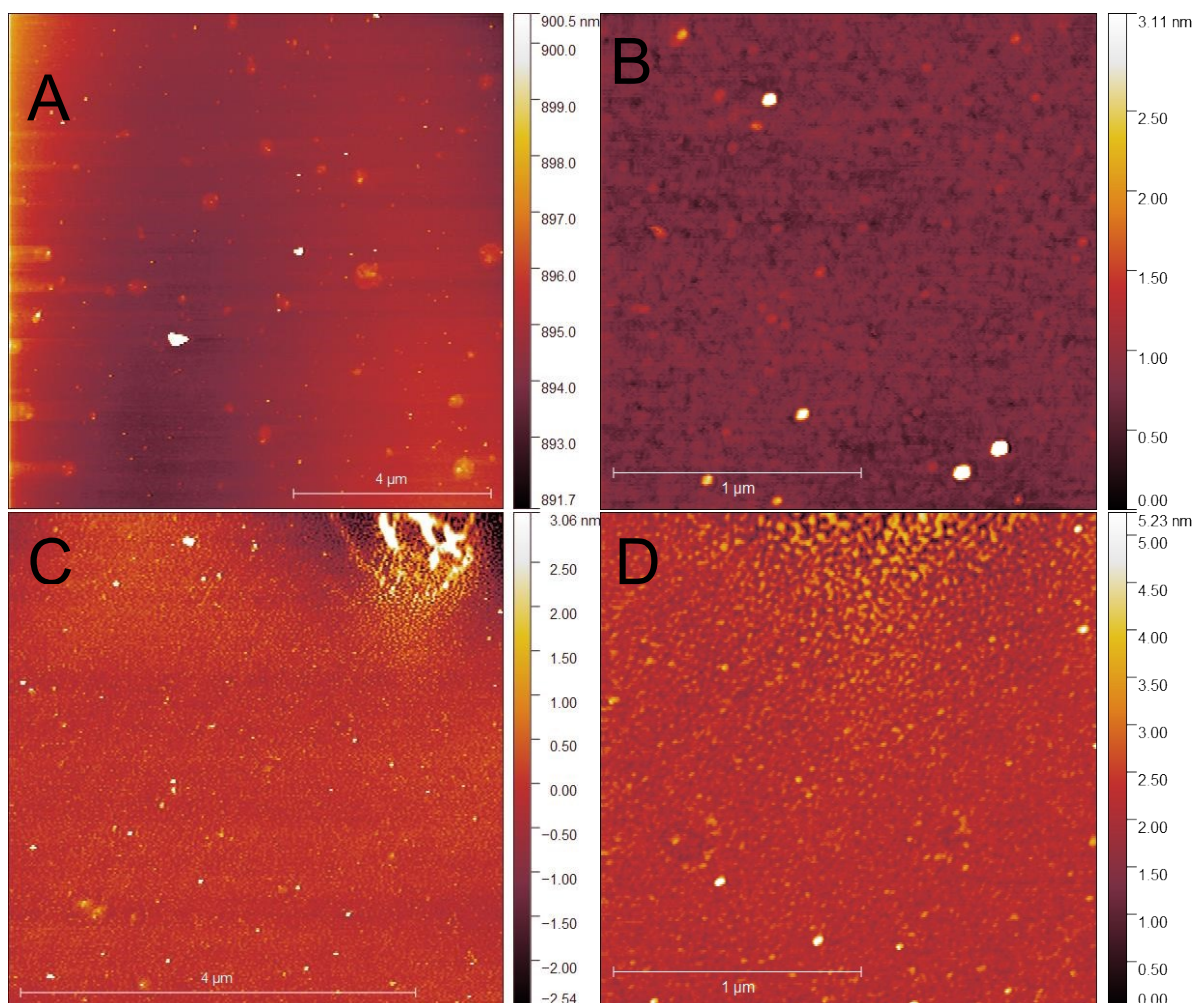


*Figure S10 AFM scans on air-plasma cleaned ALD TiO<sub>2</sub> deposited with Au<sub>101</sub> clusters using pulsed vapour deposition A,B: Sonicated, plasma cleaned ALD TiO<sub>2</sub> C,D: Same sample measured directly after 10x pulses of 0.125mM Au<sub>55</sub> solution*

Au<sub>110/55</sub> gold clusters were deposited onto ALD TiO<sub>2</sub> in a test of the potential use of pulsed vapour deposition for other cluster types. The solution used for deposition was 0.1mM Au<sub>55</sub> nanoclusters in Dichloromethane (used for its favourable solvation of these clusters). The Au<sub>55</sub> cluster size has been reported to be around 1.3-1.5 nm (Kim, Oh et al. 2004), larger than Au<sub>9</sub>. ALD TiO<sub>2</sub> was used instead of Mica as the effectiveness of depositions onto photocatalytic substrate was of interest and the larger clusters were still discernible despite the increased surface roughness. Surface roughness increased from RMS (Sq) = 212.9 nm in O<sub>2</sub> plasma cleaned, undeposited samples to RMS (Sq) = 337.0 nm when averaged across 2 μm scan regions.